THE JOURNAL OF PHYSICAL CHEMISTRY C

Article

pubs.acs.org/JPCC

Remarkable Hydrogen Storage on Beryllium Oxide Clusters: First-Principles Calculations

Ravindra Shinde*[,†] and Meenakshi Tayade[‡,§]

[†]Department of Physics, Indian Institute of Technology Bombay, Mumbai, Maharashtra 400076, India

[‡]Department of Chemistry, Institute of Chemical Technology, Mumbai, Maharashtra 400019, India

Supporting Information

ABSTRACT: Since the current transportation sector is the largest consumer of oil, and subsequently responsible for major air pollutants, it is inevitable to use alternative renewable sources of energies for vehicular applications. The hydrogen energy seems to be a promising candidate. To explore the possibility of achieving a solid-state high-capacity storage of hydrogen for onboard applications, we have performed first-principles density functional theoretical calculations of hydrogen storage properties of beryllium oxide clusters $(BeO)_n$ (n = 2−8). We observed that a polar BeO bond is responsible for H_2 adsorption. The problem of cohesion of beryllium atoms does not arise, as they are an integral part of BeO clusters. The $(BeO)_n$ (n = 2−8) adsorbs 8−12 H_2 molecules with an adsorption energy in the desirable range of reversible hydrogen storage. The gravimetric density of H_2 adsorbed on BeO clusters meets the ultimate 7.5 wt % limit, recommended for onboard practical applications. In conclusion, beryllium oxide clusters exhibit a remarkable solid-state hydrogen storage.

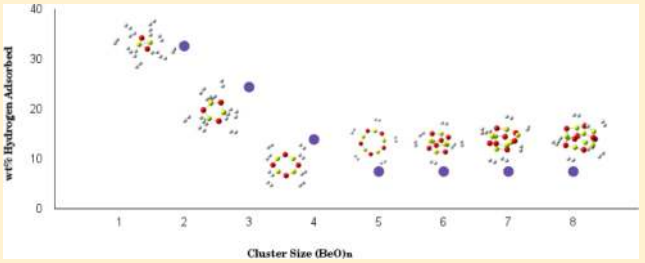

1. INTRODUCTION

Hydrogen energy has emerged as a clean, highly efficient, and eco-friendly option to fossil fuels.[1−8] Hydrogen fuel delivers a very high energy per unit mass as compared to other fuels. However, the utilizable energy per unit volume is very low. Cryogenic liquid hydrogen or high-pressure hydrogen cylinder can achieve high volumetric densities. Such a storage may not be the safe option for vehicular applications. For practical onboard applications, hydrogen needs to be stored at optimum pressures and temperatures with easy reversibility and fast kinetics.[9,10] The use of hydrogen as a fuel is hindered by the lack of economical methods of its storage. A solid-state storage of hydrogen using the adsorption/desorption mechanism received a great deal of attention recently.[1−12]

Hydrogen in molecular form tries to physisorb on the substrate surface rather weakly, and in atomic form, it chemisorbs strongly with substrate material. In the former case, a low hydrogen storage is achieved with hydrogen desorbing easily, and in the latter, a high storage is achieved, but desorption of H_2 is more difficult.[9,11] For an efficient and reversible hydrogen storage medium, it is advisible to have hydrogen adsorbed in molecular form with adsorption energy in the range 0.1−0.4 eV/H_2.[9−11,13] A potential storage material of H_2 would have a large surface area and low molecular weight. The US Department of Energy (DOE) has set an ultimate goal that the gravimetric density of H_2 should exceed 7.5 wt %.[14]

A natural choice of adsorbent material would be materials containing light elements. There has been an enormous exploration of possibilities of having carbon based, boron based, and other doped materials that can store a significant amount of hydrogen. For example, metal based hydrides have been studied extensively.[3,8,9,12,15−20] However, in this case, the gravimetric weight percentage is quite low and also the hydrogen tries to chemisorb on the transition metals. This needs higher operating temperatures to desorb hydrogen. Carbon based structures in various forms have also been studied widely. Carbon foams, hydrogen filled carbon nanotubes, graphene, graphane sheets, boron-nitride fullerenes, etc., are a few representative examples.[4,9,11−13,21−29] However, pure carbon based materials are found to adsorb hydrogen very weakly.[21−23] Low operating temperatures prohibit practical use of the metal−organic framework (MOF) hydrogen adsorbents.[1,5,6,30] Transition metal decorated fullerenes have the potential of high-capacity hydrogen storage,[31] but cohesion of decorated transition metals is still a problem. The metal adsorption energy needs to be larger than the cohesive energy of transition metal atoms. To bypass the problem of cohesion of metal atoms, adsorbing hydrogen directly on a substrate is preferred.[32] Hence, in this paper, we systematically investigate the high-capacity hydrogen storage behavior of beryllium oxide clusters using first-principles density functional calculations. These clusters are studied extensively and are found to be very stable.[33] Since hydrogen adsorbs directly on these clusters, the cohesion problem is eliminated. Also, the base clusters consist of only lightweight elements, making hydrogen gravimetric density quite larger than those of transition metal based

Received: November 8, 2013
Revised: June 20, 2014
Published: June 25, 2014

dx.doi.org/10.1021/jp4109943 | J. Phys. Chem. C 2014, 118, 17200−17204

substrates. A correlation of hydrogen adsorption energies per H_2, maximum possible hydrogen wt %, and incremental binding energies with respect to the increasing size of the beryllium oxide cluster has been presented. This work may help in experimental realization of high-capacity, sustainable hydrogen fuels, which is a need of today's and coming generations.

The remainder of the paper is organized as follows. Section 2 describes details of the first-principles calculations, followed by section 3, in which results are presented and discussed. In section 4, we present conclusions and discuss future implementation.

2. COMPUTATIONAL DETAILS

All first-principles density functional theoretical calculations were performed using Gaussian 09 code.[34] Geometries of both bare and hydrogen adsorbed BeO clusters were optimized without any symmetry constraints using the gradient embedded genetic algorithm (GEGA).[35−37] In this method, initial geometries of species in the population are randomly generated in one, two, and three dimensions. The population size is taken as $5N$, where N is the number of atoms in the cluster. All structures in this initial population are optimized to the nearest local minimum using Gaussian 09 code using a smaller basis set. All successfully converged local minimum structures undergo breeding and mutations. Structures with low overall energies are preferred for breeding with probabilities depending on their energies. Couples of parents are randomly selected for breeding based on these probabilities. A random plane cuts through both parents. The resultant half structures are then joined, forming a child; i.e., the part above the cutting plane of parent 1 is combined with the part below the cutting plane of parent 2, keeping the number of atoms the same. Such structures are again optimized to the nearest local minimum. This random selection of parents is continued until the population gets doubled, i.e., N initial parents plus N newborn children. These $2N$ structures are sorted according to their energies, and a new set of N low-lying structures is formed. If the lowest energy structure in each iteration of breeding remains the lowest for 20 iterations, then the algorithm is said to be converged to the global minimum. Structures with higher energies are selected for mutations. The structures of one-third population are randomly kicked out of equilibrium and then converged to the nearest minimum. This prevents trapping of species in a particular local minimum. The mutants are added to the population along with their precursors, and the breeding iterations continue. After convergence, the lowest energy structure and various low-lying structures are optimized with a larger basis set at a higher level of theory.

We used the ωB97xD energy functional along with an all-electron 6-311+G(d, p) basis set for the final optimization. The effect of van der Waals interactions was included explicitly by using the empirical correction scheme of Grimme (DFT +D2).[38] On the global minimum structures of BeO clusters, a number of H_2 molecules were successively added, and the structures were reoptimized. This procedure was repeated until hydrogen remained adsorbed or the adsorption energy fell below 0.10 eV/H_2. This ensured that H_2 remains physisorbed and feasible for reversible adsorption operational conditions.

3. RESULTS AND DISCUSSION

In this section, we present the results of first-principles calculations, organized as follows. The following subsection presents the geometrical structures and stability of BeO clusters, followed by the electronic structure of bare and hydrogen-decorated BeO clusters. In the final subsection, we discuss the hydrogen storage ability of BeO clusters.

3.1. Structures and Binding Energies. In order to make sure that the adsorbent BeO clusters are stable, we calculated binding energies using the following formula

$$E_b = -\frac{[E(\mathrm{BeO})_n - n \times E(\mathrm{BeO})]}{n} \quad (1)$$

where $E(\mathrm{BeO})_n$ and $E(\mathrm{BeO})$ represent the total energies of the $(\mathrm{BeO})_n$ cluster and a single BeO molecule, respectively. If the value of E_b is positive, it means that the cluster formation is exothermic and therefore stable. The various isomers of a given cluster, which are metastable, have not been considered here because the global minimum structure is the most favored if produced experimentally.

The binding energy of the clusters (E_b) and increment in the binding energy $\Delta E_b = E_b(n) - E_b(n-1)$, considered in this study, are listed in Table 1. Clearly, the binding energy of the clusters increases monotonically while ΔE_b keeps on decreasing as the cluster grows. However, for the $(\mathrm{BeO})_8$ cluster, a sudden increase in ΔE_b is observed. This is mainly because of the increase in the coordination number of Be atoms, as they now bond with a greater number of oxygen atoms, thereby increasing the stability. From these results, we can conclude the following: (1) The large clusters are relatively more stable and therefore favorable. (2) The increased number of Be−O bonds in larger clusters will further help in adsorbing more hydrogen.

Table 1. Binding Energy (E_b) of (BeO_n) (n = 1−8) Clusters, Successive Difference in Binding Energy ΔE_b, Number of Hydrogen Molecules Adsorbed (N_{H_2}), Hydrogen Molecule Adsorption Weight Percentage, and the Adsorption Energy per H_2 (E_a)

n	E_b (eV)	ΔE_b (eV)	N_{H_2}	wt %	E_a (eV)
2	3.45		12	32.60	0.12
3	4.86	1.41	12	24.38	0.10
4	5.33	0.47	8	13.88	0.10
5	5.51	0.18	5	7.46	0.10
6	5.58	0.07	6	7.46	0.12
7	5.64	0.06	7	7.46	0.16
8	5.89	0.25	8	7.46	0.13

3.2. Electronic Structure. Highest occupied molecular orbitals (HOMOs) and lowest unoccupied molecular orbitals (LUMOs) of stable ground state geometries of $(\mathrm{BeO})_n$ (n = 2−8) clusters are as shown in Figure 1. HOMOs are mostly contributed from oxygen atoms, and the LUMOs are by beryllium atoms. Depending upon the geometry, one beryllium atom can bind with two or more oxygen atoms. Clusters with beryllium bound to two oxygen atoms show enhanced hydrogen adsorption behavior as compared to those bound to three or more oxygen atoms. This is mainly because of the charge transfer mechanism that polarizes the adsorbing hydrogen. For example, in the case of $(\mathrm{BeO})_2$ clusters, there is 0.14e charge transfer from each beryllium atom to each oxygen atom (Figure 2). As a result, this Be−O bond becomes polar and produces a local electric field, enough to polarize hydrogen molecules and eventually bind them to the cluster.

dx.doi.org/10.1021/jp4109943 | J. Phys. Chem. C 2014, 118, 17200−17204

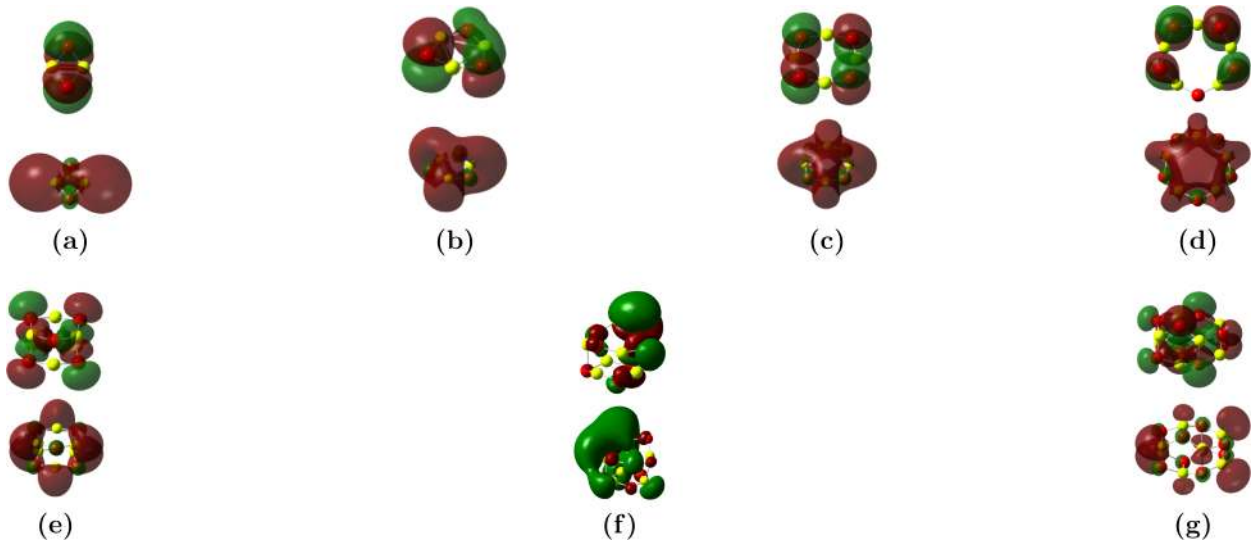

Figure 1. HOMO and LUMO corresponding to global minimum structures of $(BeO)_n$ (n = 2−8) clusters. In each subfigure, the top and bottom figures represent the HOMO and LUMO, respectively.

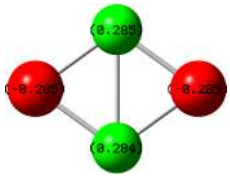

Figure 2. Mulliken charges on individual atoms of the $(BeO)_2$ cluster. Note that the polarized Be−O bond is responsible for hydrogen adsorption.

A contour plot of electrostatic potential curves in the plane of BeO units can reveal favorable docking positions of hydrogen molecules. Figure 3 shows that regions where oxygen is present,

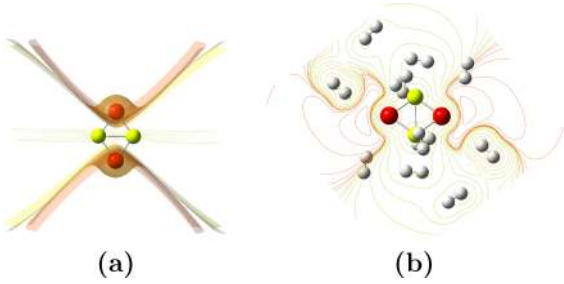

Figure 3. (a) The electrostatic potential curves due to the electronic charge density of the $(BeO)_2$ cluster. (b) The electrostatic potential contours of the $(BeO)_2$ cluster with maximum hydrogen adsorbed in the plane containing the $(BeO)_2$ cluster. Red color denotes the electrostatic potential caused due to contribution from electronic charge density of oxygen atoms, and yellow color denotes that of beryllium.

therefore, are avoided by hydrogen. This is consistent with Mulliken charge analysis that negatively charged oxygen would repel hydrogen.

3.3. Optimum Conditions for Hydrogen Storage. The affinity of hydrogen toward an adsorbent should be strong enough to store a large amount of hydrogen at charging pressures (about 30 bar) and weak enough to release most of the hydrogen at the discharging pressures (about 1.5 bar). In the Langmuir isotherm approximation, the average energy of hydrogen adsorption between pressures P_1 and P_2 is given by[10]

$$E_a = T\Delta S\gamma + \frac{RT}{2}\ln\left(\frac{P_1P_2}{P_0^2}\right) \quad (2)$$

For variety of hydrogen adsorbents, the change in entropy is $\Delta S\gamma \approx 8R$, with R being the ideal gas constant. At 298 K, with P_1 = 30 bar, P_2 = 1.5 bar, and P_0 = 1 bar, the optimum hydrogen adsorption energy equals 0.15 eV.[10] This means that, if E_a is around 0.15 eV, then the hydrogen can be adsorbed and desorbed easily in this pressure range at room temperature.

3.4. Hydrogen Storage Behavior of $(BeO)_n$ Clusters. To quantify the hydrogen uptake by $(BeO)_n$ clusters, we define hydrogen adsorption energy as

$$E_a = -\frac{[E_{(cluster+H_2)} - E_{(cluster)} - m \times E_{(H_2)}]}{m} \quad (3)$$

where $E_{(cluster+H_2)}$ is the total energy of the BeO cluster plus adsorbed hydrogens, $E_{(cluster)}$ is the total energy of the adsorbent BeO cluster, $E_{(H_2)}$ is the total energy of an individual H_2 molecule, and E_a is the hydrogen adsorption energy per H_2 molecule. The number m denotes the maximum number of H_2 molecules adsorbed on a given cluster. For $(BeO)_2$, each Be atom adsorbs six H_2, as shown in Figure 4a, which corresponds to 32.6 wt % of hydrogen adsorption. The adsorption energy is around 0.12 eV/H_2, which is in the range of reversible H_2 adsorption. The number of hydrogens adsorbed, hydrogen adsorption energies, and the gravimetric densities of all clusters studied here are listed in Table 1. The $(BeO)_3$ cluster can adsorb 12 H_2 molecules with 0.10 eV/H_2 adsorption energy obtaining 24 wt % uptake (cf. Figure 4b). A slightly different orientation of adsorbed hydrogen can lead to 18 H_2 molecules with 0.093 eV/H_2 adsorption energy, further increasing hydrogen uptake to 32.6 wt %. With 0.10 eV/H_2 adsorption energy, $(BeO)_4$ can adsorb up to 8 H_2, giving 14 wt % gravimetric density (cf. Figure 4c). Clusters $(BeO)_n$, with n = 5−8 (cf. Figure 4d−g), adsorb an equal number of H_2 as that of Be, giving rise to the same gravimetric density of 7.46 wt %. The hydrogen adsorption energy lies in the range 0.10−0.16

dx.doi.org/10.1021/jp4109943 | J. Phys. Chem. C 2014, 118, 17200−17204

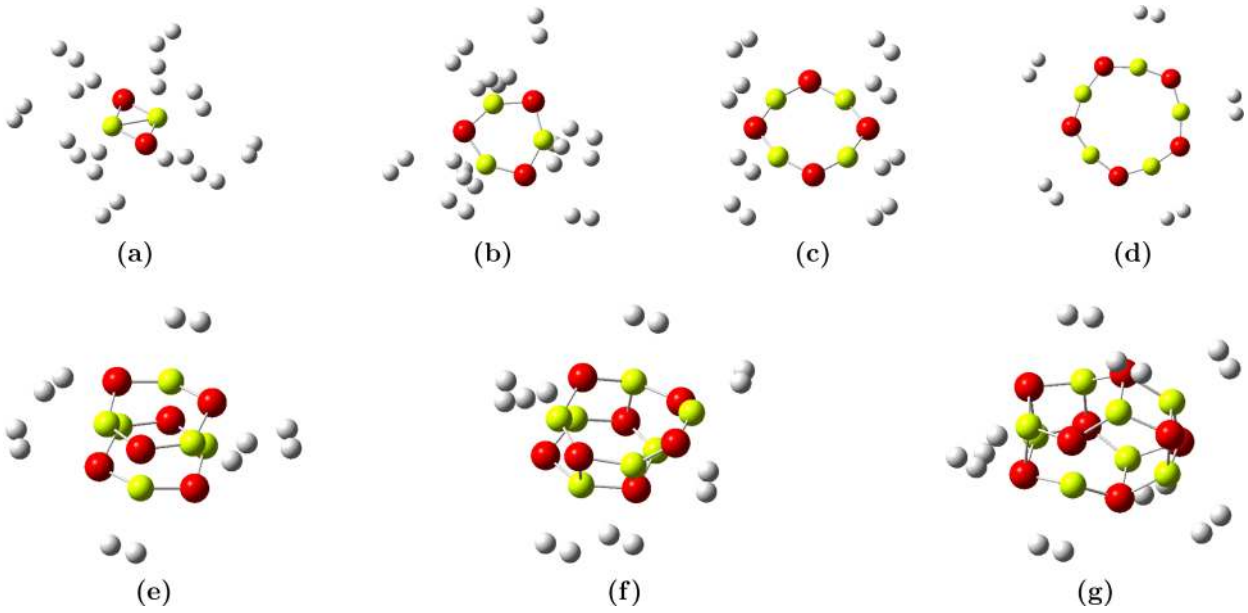

Figure 4. Geometry optimized global minimum structures of $(BeO)_n$ (n = 2−8) clusters with adsorbed hydrogen. Red, yellow, and gray colors denote oxygen, beryllium, and hydrogen atoms, respectively.

eV/H_2. It is noted that the number of hydrogens adsorbed decreases with an increase in the cluster size. This is mainly due to the steric hindrance as well as reduced charge-transfer effect. Also, an increased coordination number of Be atoms in the cluster causes the hydrogen adsorption energy to be slightly on the higher side.

Since smaller clusters are favorable for high hydrogen uptake, these clusters can be used for devising efficient high-capacity hydrogen storage materials. Carbon foams and large nanotubes are found to adsorb H_2 with low wt %.[18,21−23,39] The BeO clusters can be embedded in porous nanostructures or can be supported on MOF to achieve large-scale hydrogen adsorption; however, such embedding would reduce the overall wt % of hydrogen adsorption.

4. CONCLUSIONS AND OUTLOOKS

Using first-principles calculations, we show that a remarkable high-capacity hydrogen storage can be achieved on $(BeO)_n$ clusters. The choice of using BeO clusters naturally avoids the aggregation problem usually found in metal-on-substrate type hydrogen adsorbents, as the Be are part of the substrate itself. The polar nature of the Be−O bond—caused due to electronic charge transfer from Be to O—induces an electric field around the positively charged Be atom which in turn polarizes H_2 and adsorbs them. The adsorption energies of H_2 are within 0.10−0.16 eV/H_2, which is a recommended range for reversible hydrogen physisorption under standard test conditions. This study may stimulate experimental efforts to check the claims of high-capacity, stable, reversible hydrogen adsorption, reported here.

■ ASSOCIATED CONTENT

Supporting Information

The Cartesian coordinates of geometry optimized bare and hydrogen-adsorbed beryllium oxide clusters with few low-lying isomers are presented. The total energy and relative energies of isomers of these clusters are also given. This material is available free of charge via the Internet at http://pubs.acs.org.

■ AUTHOR INFORMATION

Corresponding Author

*E-mail: ravindra.shinde@iitb.ac.in. Phone: +91 (0)22 25764558. Fax: +91 (0)22 25767552.

Notes

The authors declare no competing financial interest.

§M.T.: E-mail: mkstayade@gmail.com.

■ ACKNOWLEDGMENTS

R.S. thanks the Council of Scientific and Industrial Research (CSIR), India, for a research fellowship (09/087/(0600) 2010-EMR-I). The authors kindly acknowledge useful discussions with Dr. Garima Jindal.

■ REFERENCES

(1) Rowsell, J. L. C.; Yaghi, O. M. Effects of Functionalization, Catenation, and Variation of the Metal Oxide and Organic Linking Units on the Low-Pressure Hydrogen Adsorption Properties of Metal-Organic Frameworks. *J. Am. Chem. Soc.* **2006**, *128*, 1304−1315.

(2) Lueking, A.; Yang, R. T. Hydrogen Spillover from a Metal Oxide Catalyst onto Carbon Nanotubes−Implications for Hydrogen Storage. *J. Catal.* **2002**, *206*, 165−168.

(3) Kaye, S. S.; Long, J. R. Hydrogen Storage in the Dehydrated Prussian Blue Analogues $M_3[Co(CN)_6]_2$ (M = Mn, Fe, Co, Ni, Cu, Zn). *J. Am. Chem. Soc.* **2005**, *127*, 6506−6507.

(4) Seayad, A. M.; Antonelli, D. M. Recent Advances in Hydrogen Storage in Metal-Containing Inorganic Nanostructures and Related Materials. *Adv. Mater.* **2004**, *16*, 765−777.

(5) Li, Y.; Yang, R. T. Hydrogen Storage in Metal-Organic Frameworks by Bridged Hydrogen Spillover. *J. Am. Chem. Soc.* **2006**, *128*, 8136−8137.

(6) Li, Y.; Yang, R. T. Significantly Enhanced Hydrogen Storage in Metal-Organic Frameworks via Spillover. *J. Am. Chem. Soc.* **2006**, *128*, 726−727.

(7) Hanada, N.; Ichikawa, T.; Fujii, H. Catalytic Effect of Nanoparticle 3d-Transition Metals on Hydrogen Storage Properties in Magnesium Hydride MgH_2 Prepared by Mechanical Milling. *J. Phys. Chem. B* **2005**, *109*, 7188−7194.

(8) Kojima, Y.; Suzuki, K.-i.; Fukumoto, K.; Sasaki, M.; Yamamoto, T.; Kawai, Y.; Hayashi, H. Hydrogen Generation using Sodium

Borohydride Solution and Metal Catalyst Coated on Metal Oxide. *Int. J. Hydrogen Energy* **2002**, *27*, 1029−1034.
(9) Sun, Q.; Wang, Q.; Jena, P.; Kawazoe, Y. Clustering of Ti on a C_{60} Surface and Its Effect on Hydrogen Storage. *J. Am. Chem. Soc.* **2005**, *127*, 14582−14583.
(10) Bhatia, S. K.; Myers, A. L. Optimum Conditions for Adsorptive Storage. *Langmuir* **2006**, *22*, 1688−1700.
(11) Sun, Q.; Jena, P.; Wang, Q.; Marquez, M. First-Principles Study of Hydrogen Storage on $Li_{12}C_{60}$. *J. Am. Chem. Soc.* **2006**, *128*, 9741−9745.
(12) Zhou, J.; Wang, Q.; Sun, Q.; Jena, P. Enhanced Hydrogen Storage on Li Functionalized BC_3 Nanotube. *J. Phys. Chem. C* **2011**, *115*, 6136−6140.
(13) Hussain, T.; Pathak, B.; Maark, T. A.; Araujo, C. M.; Scheicher, R. H.; Ahuja, R. Ab Initio Study of Lithium-Doped Graphane for Hydrogen Storage. *Europhys. Lett.* **2011**, *96*, 27013.
(14) http://www1.eere.energy.gov/hydrogenandfuelcells/storage/pdfs/targets_onboar_hydro_storage.pdf, 2009.
(15) Koukaras, E. N.; Zdetsis, A. D.; Sigalas, M. M. Ab Initio Study of Magnesium and Magnesium Hydride Nanoclusters and Nanocrystals: Examining Optimal Structures and Compositions for Efficient Hydrogen Storage. *J. Am. Chem. Soc.* **2012**, *134*, 15914−15922.
(16) Wagemans, R. W. P.; van Lenthe, J. H.; de Jongh, P. E.; van Dillen, A. J.; de Jong, K. P. Hydrogen Storage in Magnesium Clusters: Quantum Chemical Study. *J. Am. Chem. Soc.* **2005**, *127*, 16675−16680.
(17) Srinivasu, K.; Ghosh, S. K.; Das, R.; Giri, S.; Chattaraj, P. K. Theoretical Investigation of Hydrogen Adsorption in All-Metal Aromatic Clusters. *RSC Adv.* **2012**, *2*, 2914−2922.
(18) Singh, A. K.; Lu, J.; Aga, R. S.; Yakobson, B. I. Hydrogen Storage Capacity of Carbon-Foams: Grand Canonical Monte Carlo Simulations. *J. Phys. Chem. C* **2011**, *115*, 2476−2482.
(19) Kelkar, T.; Pal, S.; Kanhere, D. G. Density Functional Investigations of Electronic Structure and Dehydrogenation Reactions of Al- and Si-Substituted Magnesium Hydride. *ChemPhysChem* **2008**, *9*, 928−934.
(20) Kelkar, T.; Pal, S. A Computational Study of Electronic Structure, Thermodynamics and Kinetics of Hydrogen Desorption from Al- and Si-Doped α-, γ-, and β-MgH_2. *J. Mater. Chem.* **2009**, *19*, 4348−4355.
(21) Dodziuk, H.; Dolgonos, G. Molecular Modeling Study of Hydrogen Storage in Carbon Nanotubes. *Chem. Phys. Lett.* **2002**, *356*, 79−83.
(22) Shiraishi, M.; Takenobu, T.; Ata, M. Gas-Solid Interactions in the Hydrogen/Single-Walled Carbon Nanotube System. *Chem. Phys. Lett.* **2003**, *367*, 633−636.
(23) Kajiura, H.; Tsutsui, S.; Kadono, K.; Kakuta, M.; Ata, M.; Murakami, Y. Hydrogen Storage Capacity of Commercially Available Carbon Materials at Room Temperature. *Appl. Phys. Lett.* **2003**, *82*, 1105−1107.
(24) Li, C.; Li, J.; Wu, F.; Li, S.-S.; Xia, J.-B.; Wang, L.-W. High Capacity Hydrogen Storage in Ca Decorated Graphyne: A First-Principles Study. *J. Phys. Chem. C* **2011**, *115*, 23221−23225.
(25) Wu, H.; Fan, X.; Kuo, J.-L. Metal Free Hydrogenation Reaction on Carbon Doped Boron Nitride Fullerene: A DFT Study on the Kinetic Issue. *Int. J. Hydrogen Energy* **2012**, *37*, 14336−14342.
(26) Naumkin, F. Y.; Wales, D. J. H_2 Molecules Encapsulated in Extended Be_n Cluster Cages: Toward Light-Metal Nanofoams for Hydrogen Storage. *J. Phys. Chem. A* **2011**, *115*, 12105−12110.
(27) Li, J.; Hu, Z.; Yang, G. High-Capacity Hydrogen Storage of Magnesium-Decorated Boron Fullerene. *Chem. Phys.* **2012**, *392*, 16−20.
(28) Wu, H.-Y.; Fan, X.; Kuo, J.-L.; Deng, W.-Q. DFT Study of Hydrogen Storage by Spillover on Graphene with Boron Substitution. *J. Phys. Chem. C* **2011**, *115*, 9241−9249.
(29) Oku, T.; Kuno, M.; Narita, I. Hydrogen Storage in Boron Nitride Nanomaterials Studied by TG/DTA and Cluster Calculation. *J. Phys. Chem. Solids* **2004**, *65*, 549−552.
(30) Han, S. S.; Mendoza-Cortes, J. L.; Goddard, W. A., III Recent Advances on Simulation and Theory of Hydrogen Storage in Metal-Organic Frameworks and Covalent Organic Frameworks. *Chem. Soc. Rev.* **2009**, *38*, 1460−1476.
(31) Dixit, M.; Adit Maark, T.; Ghatak, K.; Ahuja, R.; Pal, S. Scandium-Decorated MOF-5 as Potential Candidates for Room-Temperature Hydrogen Storage: A Solution for the Clustering Problem in MOFs. *J. Phys. Chem. C* **2012**, *116*, 17336−17342.
(32) Wang, Y.; Li, X.; Wang, F.; Xu, B.; Zhang, J.; Sun, Q.; Jia, Y. Li_2O Clusters for High-Capacity Hydrogen Storage: A First Principles Study. *Chem. Phys.* **2013**, *415*, 26−30.
(33) Ren, L.; Cheng, L.; Feng, Y.; Wang, X. Geometric and Electronic Structures of $(BeO)_n$ (n = 2−12, 16, 20, and 24): Rings, Double Rings, and Cages. *J. Chem. Phys.* **2012**, *137*, 014309.
(34) Frisch, M. J.; et al. *Gaussian 09*, revision A.02; Gaussian, Inc.: Wallingford, CT, 2009.
(35) Alexandrova, A. N.; Boldyrev, A. I.; Fu, Y.-J.; Yang, X.; Wang, X.-B.; Wang, L.-S. Structure of the $Na_xCl_{x+1}^-$ (x = 1−4) Clusters via Ab Initio Genetic Algorithm and Photoelectron Spectroscopy. *J. Chem. Phys.* **2004**, *121*, 5709−5719.
(36) Olson, J. K.; Boldyrev, A. I. Ab Initio Search for Global Minimum Structures of the Novel B_3H_y (y = 4−7) Neutral and Anionic Clusters. *Inorg. Chem.* **2009**, *48*, 10060−10067.
(37) Alexandrova, A. N.; Boldyrev, A. I. Search for the $Li_n^{0/+1/-1}$ (n = 5−7) Lowest-Energy Structures Using the Ab Initio Gradient Embedded Genetic Algorithm (GEGA). Elucidation of the Chemical Bonding in the Lithium Clusters. *J. Chem. Theory Comput.* **2005**, *1*, 566−580.
(38) Grimme, S. Semiempirical GGA-Type Density Functional Constructed with a Long-Range Dispersion Correction. *J. Comput. Chem.* **2006**, *27*, 1787−1799.
(39) Liu, C.; Chen, Y.; Wu, C.-Z.; Xu, S.-T.; Cheng, H.-M. Hydrogen Storage in Carbon Nanotubes Revisited. *Carbon* **2010**, *48*, 452−455.